

Modeling Resonant Wavelengths for Type II “W” Optical Pumping Injection Cavity Lasers

Lauren Ice and Dr. Linda Olafsen

Abstract— Optical pumping injection cavity lasers allow for multiple passes through the active region, which increases conversion efficiencies and threshold density. For these lasers to work efficiently, they have to be pumped at the resonance wavelength for the laser cavity.[1-5] In this paper, the reflectance as a function of wavelength for a laser structure is modeled and the resonance found. The resonance wavelength dependence on the temperature, in which the laser is operating, is investigated by adjusting the linear temperature dependence of the indices of refraction of the compounds in the active region and temperature gradient throughout the laser structure. This is then compared to experimental data. It is found that the linear temperature dependence of the indices of refraction of the compounds in the active region and/or the overall temperature gradient in the structure increases with temperature and pump intensity. This is due to an increase in pump intensity at higher temperatures, which induces a temperature gradient and increases the index of refraction in the active region.

I. INTRODUCTION

Efficient lasers, which emit in the mid-infrared region at room temperature, are needed for a wide variety of applications including chemical detection for medical, environmental and defense purposes.[4] Two important parameters to look at when evaluating a lasers performance are the external differential quantum efficiency and threshold carrier density. External differential quantum efficiency is the ratio of photons emitted from the laser to the number of injected pump carriers and is the slope of the input carriers vs. light emitted curve shown in *Figure 1*. This depends on the internal differential quantum efficiency, which is the percentage of injected pump carriers that are converted into photons inside the cavity, and the internal loss, which is the

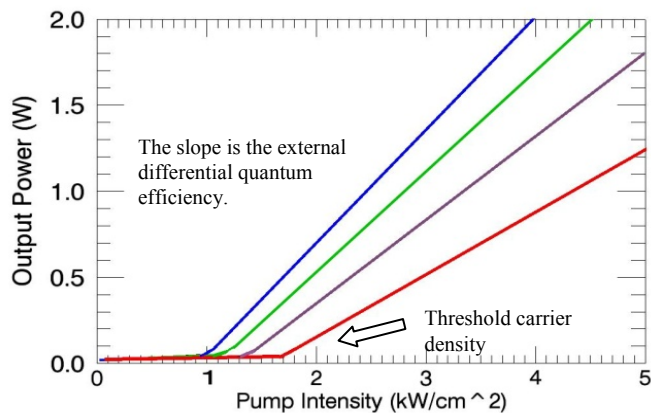


Figure 1. Output Power vs. Pump intensity. The external differential quantum efficiency is the slope of the curves. I_{th} is the threshold intensity. The different slopes represent different pump wavelengths.

amount of photons reabsorbed into the quantum wells before they can be emitted. The threshold carrier density is the intensity of injected pump carriers where stimulated emission begins, also shown *Figure 1*. [6]

One method to obtain high external differential quantum efficiency and low threshold carrier density is with Optical Pumping Injection Cavity (OPIC) lasers with a type II “W” active region. OPIC lasers are optically pumped instead of electrically driven and are made of an active quantum well region, surrounded by spacer and hole-blocking layers and then by Distributed Bragg Reflector (DBR) mirrors. DBR mirrors consist of alternating layers of media with high and low dielectric constants and because of the DBR mirrors, when the etalon cavity is pumped at resonance, it provides the pump photons multiple passes through the active region. This causes pump absorption to increase per quantum well and simultaneously lowers the threshold carrier density, thus requiring fewer quantum wells. Having fewer quantum wells decreases the internal loss or re-absorption of the radiation within the cavity, providing higher external differential quantum efficiency and low threshold carrier density.[1-5]

To find the resonant pump wavelength of the laser, the theory of multilayer films is used. From this, the reflectance as a function of wavelength for a given structure can be found. At each interface of two media within the structure, the component normal to the interface, of both the electric and magnetic fields must be continuous. For a single layer of film, an electromagnetic wave with an electric field of E_0 , passes from an initial index of n_0 to the film, of thickness, l and refractive index of refraction, n_1 and then to another material with index n_T . E_1 is the electric field in the film and E_T is the transmitted electric field. At each interface, part of the initial electromagnetic wave is transmitted and part is reflected. This is shown below in *Figure 2*.

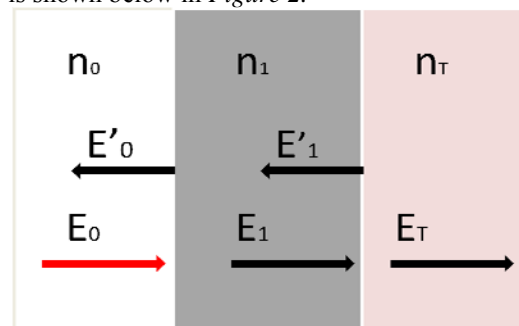


Figure 2, shows reflection and transmission of an initial electric field, E_0 going from an initial medium with index n_0 to a second medium of index n_1 . There the primed are the reflected fields and E_T is the transmitted electric field.

Equation 1 and Equation 2, below, represent the continuity of both the electric and magnetic fields, respectively, at the first interface

$$E_0 + E'_0 = E_1 + E'_1 \quad \text{Equation 1}$$

$$n_0 E_0 - n_0 E'_0 = n_1 E_1 - n_1 E'_1 \quad \text{Equation 2}$$

And for the second interface,

$$E_1 e^{ikl} + E'_1 e^{-ikl} = E_T \quad \text{Equation 3}$$

$$E_1 n_1 e^{ikl} - E'_1 n_1 e^{-ikl} = n_T E_T \quad \text{Equation 4}$$

Where all of the reflected electric fields are primed and k is the wave number and is given by $2\pi n_0/\lambda$.

From these boundary conditions, the coefficients for both the reflectance, $r = \frac{E'_0}{E_0}$ and the transmittance, $t = \frac{E_T}{E_0}$ can be found. In matrix form,

$$\begin{bmatrix} 1 \\ n_0 \end{bmatrix} + \begin{bmatrix} 1 \\ -n_0 \end{bmatrix} r = M \begin{bmatrix} 1 \\ n_T \end{bmatrix} t \quad \text{Equation 5}$$

where

$$M = \begin{bmatrix} \cos(kl) & \frac{-i}{n_1} \sin(kl) \\ -in_1 \sin(kl) & \cos(kl) \end{bmatrix} \quad \text{Equation 6}$$

The matrix, M , is called the transfer matrix. The boundary conditions at each interface in a multilayer film can be represented by a transfer matrix. From the product of all of the transfer matrices for a structure, the total coefficient of reflectance can be found. Assigning each element from the final transfer matrix a letter A through D, as follows,

$$M = \begin{bmatrix} A & B \\ C & D \end{bmatrix} \quad \text{Equation 7}$$

the coefficients of reflectance and transmittance can be found.

$$r = \frac{An_0 + Bn_0 n_T - C - Dn_T}{An_0 + Bn_0 n_T + C + Dn_T} \quad \text{Equation 8}$$

$$t = \frac{2n_0}{An_0 + Bn_0 n_T + C + Dn_T} \quad \text{Equation 9}$$

And, finally the reflectance, R and the transmittance, T are,

$$R = |r|^2 \quad \text{Equation 10}$$

And

$$T = |t|^2 \quad \text{Equation 11}$$

Each transfer matrix, and therefore the reflectance, is a function of pump wavelength as well as the thickness and index of refraction of each layer. For many layer films, there is a region of wavelengths, all of which have a reflectance close to unity.[7]

For an OPIC laser, this reflectance “plateau” in the reflectance curves has a small notch in it where there is partial transmittance. Shown in Figure 3. This is from the cavity between the mirrors.

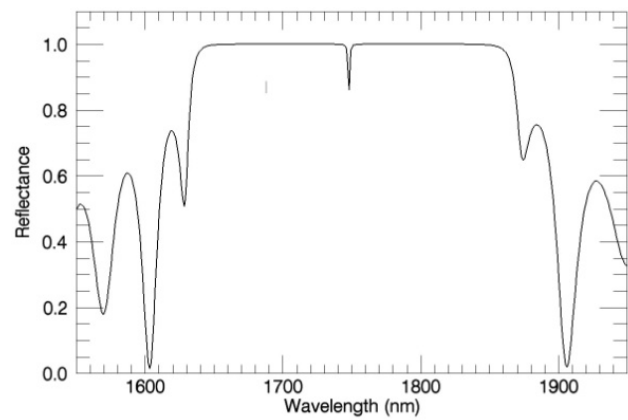


Figure 3. Reflectance as a function of Wavelength. The “plateau” where the reflectance is close to unity is produced from the DBR mirrors and the “notch” is the resonant wavelength of the cavity.

This small “notch” (shown in Figure 3) is the resonance of the structure and the ideal pumping wavelength. The resonance wavelength of a particular laser structure’s cavity depends on the temperature at which the laser is operating and the intensity of the pump beam. Temperature changes the lattice constant of the compounds in which the laser is built, therefore changing the thickness of the individual layers. [8-10] Also, the index of refraction of the layers has temperature dependence, as follows,

$$\frac{dn}{ndT} = \alpha \quad \text{Equation 12}$$

Where α is the linear coefficient of index of refraction change with temperature. This gives a positive increase in the index of refraction as the temperature rises. Also, an increase in temperature decreases gain and with it, the index of refraction within the active region of the laser. [11] Because of this, at higher temperatures, the laser is pumped at greater intensities. This higher optical intensity increases the indices of refraction of the compounds in the active region.

Experimentally, the temperature dependence of the resonant wavelength is parabolic. This dependence has not been well investigated or modeled. To be able to do this allows for room temperature operation lasers to be built and resonantly pumped, increasing efficiency.

II. EXPERIMENT

This experiment was to model the resonance wavelength of an OPIC laser as a function of temperature. The structure that was modeled, is the one discussed in references 3 through 5. The structure consisted of an active region of 10 periods of 2.1 nm of InAs, 3.4 nm of GaSb, another layer of 2.1 nm of InAs and a 4.0 nm layer of AlSb. This was surrounded by a 10.0 nm layer of AlAs_{0.08}Sb_{0.92} hole-blocking layers and 521.3 nm GaSb spacer layers and then 10 periods (top) and 18.5 periods (bottom) of the DBR mirrors. These were made from alternating layers of 175.8 nm AlAs_{0.08}Sb_{0.92} and 145.1 nm GaSb. The temperature, which ranged from 78 K to 325 K during the experiment, was controlled through a copper block on which the laser was mounted. Experimentally, the laser has resonance as a function of block temperature as shown in Figure 4.

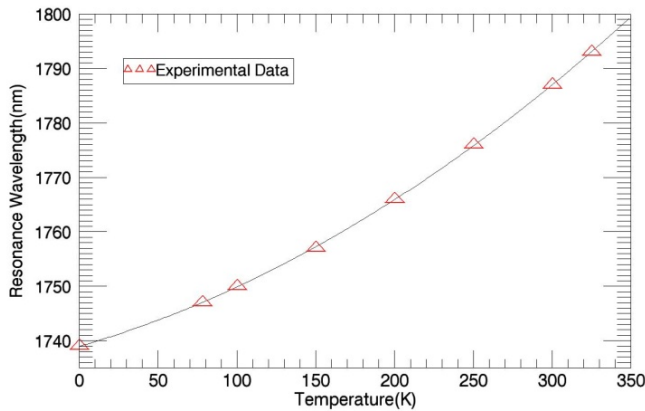


Figure 4. The triangles indicate the experimental data for the resonance wavelength as a function of temperature for the OPICR00323 structure. The curve is parabolic and is given by

$$\text{Resonant wavelength (nm)} = 1739.97 \text{ (nm)} + 0.0838167 \text{ (nm/K)}(\text{temp(K)}) + 0.000254427 \text{ (nm/K}^2\text{)}(\text{temp(K)})^2$$

Interactive Data Language (IDL) is used for the modeling and the program consists of a master program and three other programs. The master program defines the block temperature array, with temperatures from 0 K to 325 K, as well as, made variations in the index of refraction temperature gradient, α , in Equation 12 and a variable temperature gradient in the structure. This program then calls three other programs, “structure,” “temperature” and “reflectance.” In a loop, it sends each of the block temperatures, the variation in the value α and the temperature gradient, to the three other programs.

The first program, “structure,” sets up the physical structure of the laser. It accesses files of the index of refraction as a function of wavelength, for each material, which were extrapolated from graphs of experimental findings of index of refraction change as a function of photon energy. Properties, such as the lattice constant and the linear change in lattice constant and the linear change index of refraction, α in Equation 12, as a function of temperature are input into the program at this point. The lattice constants and the linear change in lattice constant were taken from references 8, 9 and 10. For GaSb and InAs, the coefficient of linear index change is $9 \times 10^{-5} \text{ (1/K)}$ and for $\text{AlAs}_{0.08}\text{Sb}_{0.92}$ and AlSb is $5 \times 10^{-5} \text{ (1/K)}$. [12] Then, the thickness of each layer, as well as the number of periods in the region are defined. The thickness and the properties of each layer are put into an array, which is then sent to the program called “temperature.”

In “temperature,” the change in the lattice constant as a function of temperature is calculated. This changes the overall thickness of each layer as a function of temperature and replaces the original thickness values.

In the program “reflectance,” the linear changes of the index of refraction with temperature are made. Given minimum and maximum wavelengths, the program makes a transfer matrix, Equation 6, for each interface of the structure and wavelength value in nanometer steps. Each of the transfer matrices are then multiplied together and the reflectance is found using Equation 8. The program plots the reflectance as a function of wavelength for each block temperature and finds the resonance wavelength. In the master program, the

resonance wavelengths for the temperature array are plotted against the block temperature.

To minimize the error between the experimental values, shown in Figure 4, and the output from the program, the absolute value of the difference between these two, for each block temperature, is found. To account for the index of refractive changes from gain, the master program varied refractive index constant, α , for each compound by a variable multiplier. This variable, multiplier had a range of -15 to 15 in steps of 1.5 for GaSb and for each of these values it varies the AlSb index change multiplier from -20 to 20, in steps of 2.25. For each of these combinations, it varies the InAs multiplier from -15 to 15 in steps of 1.5 and prints the value of the InAs multiplier which gives the least error. By doing so, the best combinations of the changes in the refractive index are found and patterns investigated. Next, an additional variable was added to the program described above. For each combination of the indices of refraction multipliers a variable temperature gradient is added to the original plate temperature to account for heating during lasing. The variable temperature ranges from 0 K to 50 K in steps of 5 K and the temperature, which gave the least error between the experimental and the output of the program, is printed.

Throughout all of the runs, an overall thickness multiplier is used to account for deviations in the thickness of the laser structure, as taken from different areas of the wafer. This overall thickness multiplier is used to match the output of the program to the parabolic fit of the experimental data, as shown in Figure 4 at 0 K.

III. RESULTS

The overall thickness multiplier used was 0.7742. Before multiple parameters, such as index of refraction temperature dependence for the different compounds and temperature gradient, were changed together, each parameter was changed individually to match the experimental data. The linear temperature dependence for the index of refraction of each of the compounds in the active region is changed individually, and is shown below in Figure 5.

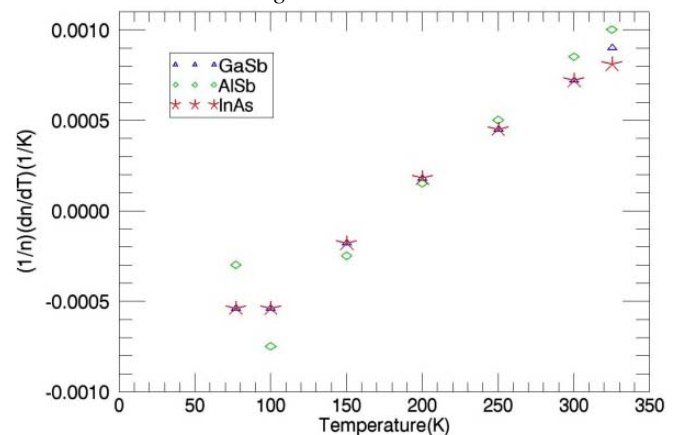


Figure 5, shows $(1/n)(dn/dT)$ as a function of temperature for each of the indices of refraction of the compounds in the active region.

This shows a general increase with increased temperature and gave the general range for program 1 described in the experiment section. When the indices of refraction were

changed in the active region together, similar patterns to *Figure 5* were found. Below, in *Figure 6* shows one of the combinations of the constant α for the compounds in the active region that would give little error between the output of the program and the experimental data show in *Figure 4*.

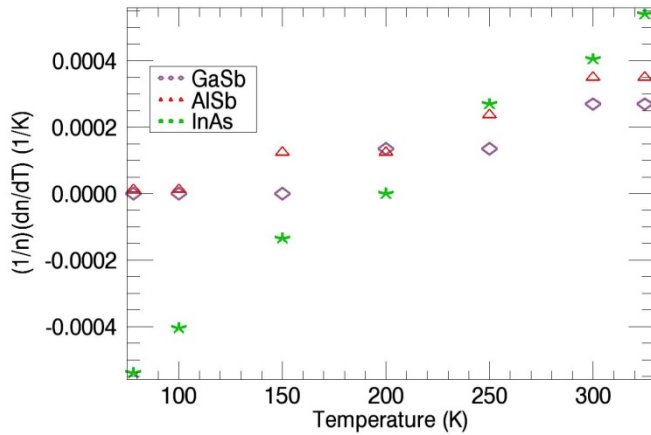


Figure 6. Index of refraction linear temperature dependence of each of the compounds in the active region as a function of time.

This figure shows a general increase in the temperature dependence of the index of refraction at higher temperatures. The changes in the temperature dependence of the index of refraction in the active region range between -0.0005 (1/K) at 0 K and 0.0005 (1/K) at 325 K. The general pattern is a linear increase.

To get the range for the next program, which changed the linear temperature dependence of the index of refraction in the active region as well as an overall temperature gradient in the laser, just the temperature was changed to fit the experimental data. This is shown below in *Figure 7*.

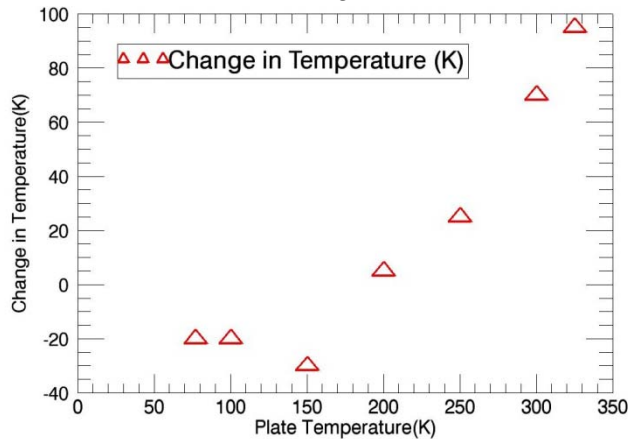


Figure 7. The triangles indicate the change in temperature from the pump beam as a function of plate temperature.

The range is from -40 to 100 , but the negative numbers were not included in the program. The results from changing the variables together are shown in *Figure 8*.

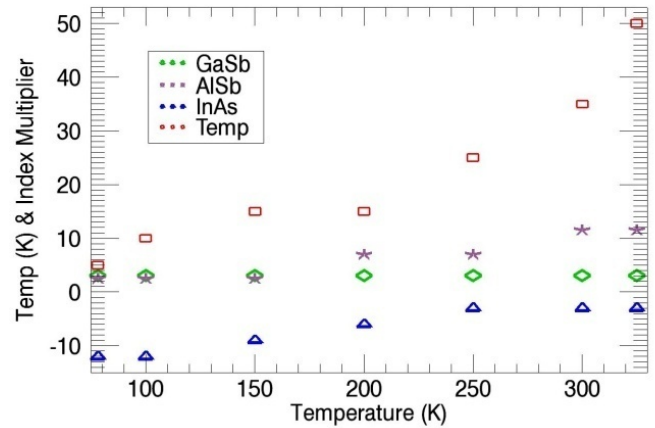


Figure 8. The multiplier on the index of refraction linear temperature dependence of the compounds in the active region and a temperature gradient as a function of plate temperature

As shown in *Figure 8* when the temperature gradient is included the changes on the index of refraction temperature dependence is smaller. The temperature is increasing in the laser, but the slope is larger at high temperatures.

IV. DISCUSSION

Overall the increase in the indices of refraction is positive and increasing. The change in the temperature dependence of the indices of refraction can be explained from the increase in pump intensity. Since gain is more difficult to achieve at higher temperatures, the laser is pumped at higher intensities. The index of refraction, as well as, gain increase with the pump intensity. [11,13] As shown in *Figure 6*, the change in InAs is the greatest. The indium arsenide layers constitute the quantum wells and cause there to be an increased change in index of refraction from the pump laser intensity.

The temperature gradient would also be produced from the increase in the pump intensity. By having an increased temperature gradient through the structure, the change in the index of refraction linear temperature dependence could be more subtle and still produce the same results. Because of the large intensities at which the pump operating, the temperature increase in the active region is very likely.

V. CONCLUSION

To fit the parabolic curve fitted to the experimental data, *Figure 4*, the linear temperature dependence of the index of refraction and/or the temperature in the laser might increase due to the increased pump intensity at higher block temperatures. By finding this change, the resonance of a laser as temperature changes can be modeled more accurately producing more efficient lasers. Goals for future research include running the programs for smaller step sizes to view more subtle changes in the index of refraction in the active region. This would allow for finding more accurate changes and allow for the dependence to be investigated more closely. Having a program with these physical changes incorporated would be ideal, because it would allow for the program to be used to make predictions on the resonant wavelength for other structures to improve their efficiency. By modeling these

lasers, their physical properties can be investigated further and efficiencies improved.

- [1] W. W. Bewley, C. L. Felix, I. Vurgaftman, D. W. Stokes, J. R. Meyer, H. Lee and R. U. Martinelli, "Optical-Pumping Injection Cavity (OPIC) Mid-IR "W" Lasers with High Efficiency and Low Loss," *IEEE Photon. Technol. Lett.*, Vol. 12, pp. 477-479, 2000.
- [2] C. L. Felix, W. W. Bewley, I. Vurgaftman, L. J. Olafsen, D. W. Stokes, J. R. Meyer and M. J. Yang, "High-efficiency midinfrared "W" laser with optical pumping injection cavity," *Applied Physics Letters*, Vol. 75, pp. 2876-2878, 1999.
- [3] T. C. McAlpine, K. R. Greene, M. R. Santilli, L. J. Olafsen, W. W. Bewley, C. L. Felix, I. Vurgaftman, J. R. Meyer, H. Lee and R. U. Martinelli, "Resonantly Pumped Optical Pumping Injection Cavity Lasers," *Journal of Applied Physics*, Vol. 96, pp. 4751-4754, 2004.
- [4] T. C. McAlpine, K. R. Greene, M. R. Santilli, L. J. Olafsen, W. W. Bewley, C. L. Felix, I. Vurgaftman, J. R. Meyer, M. J. Yang, H. Lee and R. U. Martinelli, "Pump Wavelength Tuning of Optical Pumping Injection Cavity Lasers for Enhancing Mid-Infrared Operation," *Materials Research Society Symp. Proc.*, Vol. 799, pp. 211-216, 2004.
- [5] T. C. McAlpine, L. J. Olafsen, W. W. Bewley, J. R. Meyer, I. Vurgaftman, H. Lee and R. U. Martinelli, "Transparency pump intensity, internal quantum efficiency, and internal loss in resonantly pumped W-OPIC lasers" (preprint, in preparation)
- [6] K. S. Mobarhan, "Test and Characterization of Laser Diodes: Determination of Principal Parameters," *Newport, Applications*, pp. 1-7, 1995.
- [7] G. R. Fowles, "Multiple-beam interference," in *Introduction to Modern Optics*, Second Edition New York: Dover Publications, INC., 1989, pp. 87-102.
- [8] S. Adachi, "Thermal properties," in *Properties of Group IV, III-V, and II-VI Semiconductors* England: Wiley, 2005, pp. 30.
- [9] S. Adachi. (1989, December 15, 1989). Optical dispersion relation for GaP, GaSb, InP, InAs, InSb, $\text{Al}_x\text{Ga}_{1-x}\text{As}$, and $\text{In}_{1-x}\text{Ga}_x\text{As}_y\text{P}_{1-y}$. *Journal of Applied Physics* [Online]. 66(12), pp. 6030-6040. Available: <http://link.aip.org/link/?JAP/AU/66/6030/1>
- [10] O. Madelung, "Physical data, 2 III-V compounds," in *Semiconductors-Basic Data*, 2nd revised Berlin, Germany: Springer-Verlag, 1996,
- [11] W. W. Chow and S. W. Koch, "2. free-carrier theory," in *Semiconductor Laser Fundamentals* Berlin: Springer, 1999, pp. 49-69.
- [12] I. Vurgaftman. Indices of refraction. *Indices of Refraction Linear Temperature Dependence*
- [13] D. Sands, "Optical properties of semiconductor materials," in *Diode Lasers* T. Spicer and S. Laurenson, Eds. Philadelphia: Institute of Physics Publishing, 2005, pp. 55-66.